Direct measurement of hot-carrier generation in a semiconductor barrier heterostructure: Identification of the dominant mechanism for thermal droop

Daniel J. Myers,[1] Kristina Gelžinytė,[2] Abdullah I. Alhassan,[1] Lucio Martinelli,[3] Jacques Peretti,[3] Shuji Nakamura,[1] Claude Weisbuch,[1,3] and James S. Speck[1]

[1]*Materials Department, University of California, Santa Barbara, California 93106, USA*

[2]*Institute of Photonics and Nanotechnology, Vilnius University, Sauletekio 3, 10257 Vilnius, Lithuania*

[3]*Laboratoire de Physique de la Matière Condensée, CNRS-Ecole Polytechnique, IP Paris, 91128 Palaiseau Cedex, France*

(Received 21 March 2019; published 9 September 2019)

Energy measurements of electrons emitted from a semiconductor can reveal internal physical processes hitherto elusive. Signatures of hot-electron processes in heterostructures have been observed from cesiated, light-emitting, and *p-i-n* diodes. In *p-i-n* devices with AlGaN barriers, a high-energy peak was measured and ascribed to a trap-assisted Auger recombination process. Temperature dependent measurements of light-emitting diodes with AlGaN electron blocking layers also show such hot carriers when electrons thermally reach these barriers, identifying carrier escape as the mechanism of thermal droop and demonstrating the efficacy of such barriers to partially mitigate thermal droop.

DOI: 10.1103/PhysRevB.100.125303

In most materials and structures (semiconductors, organics, phosphors, etc.), the light emission efficiency decreases with increasing temperature [1–3]. The mechanisms are varied given the range of physical phenomena leading to radiative or nonradiative recombination in such a variety of materials. In bulk semiconductors, the reduced efficiency in *photoluminescence* experiments is often attributed to Shockley-Read-Hall (SRH) nonradiative (NR) recombination [4,5]. However, in *electrically injected* diodes containing heterostructures, the "thermal droop", i.e., the decrease in internal quantum efficiency (IQE) with increasing temperature may reflect many different competing processes such as thermally activated impurity tunneling [6], temperature dependent Auger recombination [7], increased SRH recombination [8], and reduced carrier injection efficiency (η_{inj}) [8]. The analysis is challenging due to the simultaneous actions of electrical and optical phenomena, and their possible interplay. For electrical processes, one must sort out electrical injection into the optically active region, carriers overshooting this region, and carrier escape from that region. For optical processes, one has to consider linear, quadratic, and third order radiative or NR recombination processes. As a result, the origin of thermal droop in light-emitting diodes (LEDs) has not been clearly identified. Understanding the mechanism of thermal droop would open the way to its mitigation through improved heterostructure design and materials growth. We recently demonstrated, through electron emission spectroscopy (EES) from an LED, that the mechanism responsible for the efficiency droop at high current density was the interband third-order Auger process [9]. We here apply the same technique, which provides spectroscopic signatures of electronic processes and unambiguously identifies carrier overshoot as the main mechanism for thermal droop in InGaN/GaN LEDs. From these measurements, we also demonstrate the impact of electron blocking layers (EBLs) on NR recombination and carrier escape processes from the active region.

Part of the reason thermal droop in III-nitride LEDs remains an important research topic is the absence of direct measurements that reveal the carrier transport or NR recombination mechanisms responsible for this efficiency loss. Analysis of thermal droop often relies on indirect measurements of carrier dynamics by analysis of the light output power to determine changes in carrier lifetime, most commonly using of the "ABC" rate equation model for IQE where B is the radiative recombination rate, A and C are the Shockley-Read-Hall and Auger interband recombination rates, respectively. This model assumes the electron and hole concentrations being equal and constant throughout the entire active volume independently of temperature. This is a poor assumption due to several reasons, for example differences in the electron and hole mobilities leading to nonuniform injection of holes, and indium fluctuations localizing carriers to indium rich regions [10–13].

The EES technique offers a direct measurement of some of the relevant recombination and transport mechanisms occurring within the device by measuring the energy distribution of electrons that have been emitted from the surface of an electrically injected device. EES relies on negative electron affinity (NEA) achieved by deposition of a cesium monolayer on a p-type semiconductor surface, decreasing the vacuum level below the conduction band minimum making it possible for electrons to be directly emitted from the conduction bands [14–16]. The measured electron spectra can indicate changes in injection efficiency (i.e. electron overshoot and/or escape) as well as NR recombination mechanisms that result in hot-carrier generation such as interband Auger recombination [3,10,11]. A detailed schematic of the relevant energy levels, recombination mechanisms, transport phenomena and how they relate to the emitted electron energy distribution is shown in Fig. 1.

EES measurements from nitride LEDs typically show four distinct peaks. Two low-energy peaks are associated with the

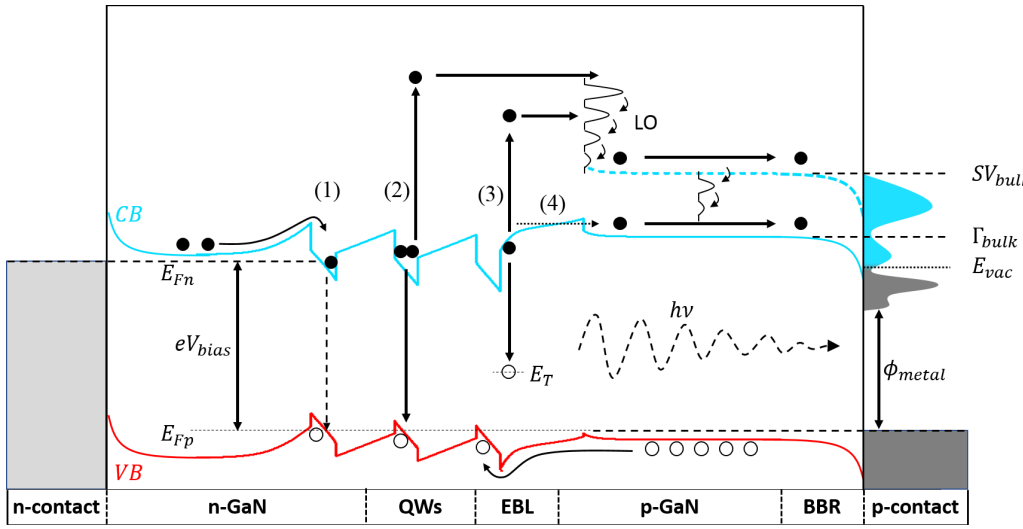

FIG. 1. Relevant electron energy levels, transport, recombination mechanisms, and the corresponding electron emission spectrum. (1) Radiative recombination, (2) interband Auger recombination, (3) TAAR in EBL, and (4) thermal escape.

light produced by the LED causing photoemission of electrons from the *p*-contact metals [17]. A mid-energy peak and a high-energy peak are associated with electrons generated within the device which have been emitted through the *p*-type semiconductor surface. The mid-energy peak corresponds to electrons that have either overshot or escaped confinement in the active region or have relaxed from higher energy states into the Γ-valley conduction band minimum before being emitted. The high-energy peak is due to hot-electron generation by the interband Auger mechanism in the LEDs active region [9,17,18] and subsequent thermalization into a conduction band side valley (SV) situated 1 eV above the Γ valley [19–21], before being emitted from the surface.

LED samples for EES have an exposed area of *p*-type GaN surface, allowing for unobstructed emission of electrons directly from the LED. EES devices were designed with a central *p* contact that includes a hexagonal array of 7-μm diameter apertures. The total injection area defined by the *p* contact is $\approx 2.2\times10^{-3}$ cm. Further details of the device design and measurements can be found in Refs. [17,22].

The electron energy was measured with a spherical sector electrostatic analyzer operated in constant pass energy mode. Because the energy reference is the Fermi level of the *p* contact, the current dependent ohmic voltage drop across the metal-semiconductor junction increases the Γ and SV peaks energies as current increases. For this reason, increasing the current through the device will also increase the measured energy of electrons emitted from the semiconductor surface whereas the low-energy photoemission peaks (which correspond to electrons photo-emitted from the contact metals) do not change with increased injection current [17].

Two *p-i-n* structures were grown, one with and one without an AlGaN EBL, by metal organic chemical vapor deposition (MOCVD). The devices consisted of a 3-μm *n*-GaN region, [Si] $= 5\times10^{18}$ cm^{-3}|125-nm unintentionally doped (UID) GaN|10-nm *p*-$Al_{0.20}Ga_{0.80}N$ EBL*, [Mg] $= 6\times10^{19}$ cm^{-3}|70-nm *p*-GaN, [Mg] $= 6\times10^{19}$ cm^{-3}| and a 10-nm *p*-GaN contact layer. The *p-i-n* structures included a 125-nm UID region to mimic the active region thickness in a typical LED. Two LED structures, one with and one without an AlGaN EBL, were grown by an industrial partner by MOCVD with *I-V* characteristics representative of commercially purchased LEDs. The structure of the LEDs includes, |Si-doped *n*-GaN region| 150 nm, low indium content InGaN region |$In_{0.18}Ga_{0.82}N$/GaN, 5× (quantum well (QW)/barrier) region |10-nm $Al_{0.20}Ga_{0.80}N$ EBL*, [Mg] $= 2\times10^{20}$ cm^{-3}|100-nm *p*-GaN, [Mg] $= 2\times10^{20}$ cm^{-3}| and a p^{++}-GaN contact layer. Additionally, two 500-nm metal samples, one palladium, one gold, were deposited on a sapphire substrate to determine how the metal low-energy photoemission peaks intensities change with increasing temperature.

To determine the integrated intensity of peaks we fit the shapes of the Γ and SV peaks by an exponentially modified Gaussian resulting from electrons thermalizing during their transit in the *p*-surface band bending region (BBR).

The conduction band energy positions in the bulk were determined from the high-energy threshold of each peak. Because electrons relax down conduction band valleys in the BBR, the highest energy electrons in each peak will have transited the BBR quasiballistically and will thus be at a bulk conduction band energy position (Fig. 1) [23].

For EES measurements to show the effects of thermal droop, it was necessary to develop a method of simultaneously measuring the changes in the LED light output and emitted electron intensities as temperature was increased. Fortunately, the EES device design has a built-in photometer, namely, the low-energy photoemission peaks due to contact metals which can be used to determine relative changes in light intensity as temperature is varied. To calibrate this, photoemission was measured on the palladium and gold film samples using a 450-nm laser, matching the LED emission wavelength. Photoemission from palladium show a large decrease in the integrated emission intensity with increasing temperature, making it a poor candidate as an in situ light meter. Conversely, the photoemission intensity from the gold remained stable in the range 21–145 °C (Fig. 2), making it an ideal photometer. This indirect light measurement does not give information on the

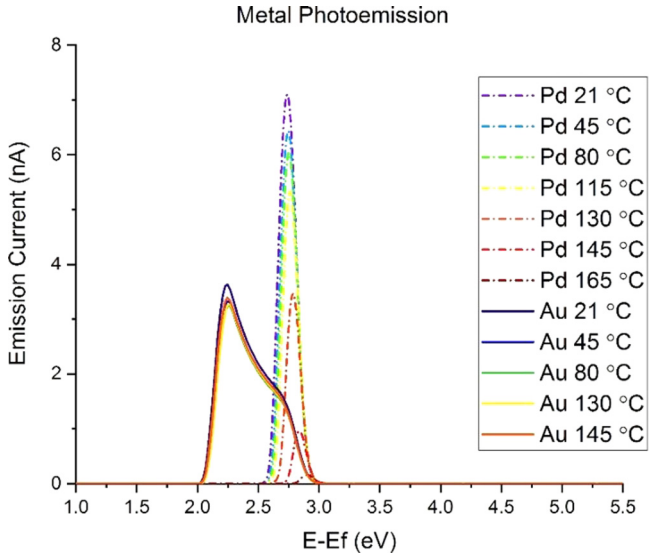

FIG. 2. Temperature dependent photoemission measurements using 4.5 mW, 450-nm laser for photoexcitation. Photoemission intensity from gold remains unchanged over the temperature range while the palladium photoemission intensity decreases with temperature.

absolute device efficiency, but still allowed for comparison of the relative changes in light output between measurements.

To understand the temperature dependent EES spectra in real-world, commercial LEDs that contain EBLs, we performed control experiments to understand the spectral contributions of the EBL in the *p-i-n* diodes with or without EBLs, and also measured the LED without an EBL.

EES measurements from a *p-i-n* structure at 25 °C are shown in Fig. 3(a). Spectra from this device were single peaked with a high-energy threshold near the expected Γ-valley minimum position (≈3.4 eV from E_F). The absence of any low-energy features indicates that the light output of this device was below the threshold for measurable photoemission from the metal contacts, not surprising for a device without any carrier confinement.

The second *p-i-n* device included a 10-nm, *p*-AlGaN EBL at the end of the UID region. Figure 3(b) shows the 25 °C energy distribution curves (EDCs) for this device at varying diode current. Two peaks were observed at all applied currents. A low-energy peak with a high-energy threshold at the expected Γ-valley position and a high-energy peak, due to hot electrons, with a high-energy threshold roughly 1 eV above the high-energy threshold of the low-energy peak. The low-energy Γ-valley peak intensity increased linearly with increasing current, like in the *p-i-n* device without the AlGaN layer. In contrast, the high-energy peak intensity increases sublinearly with diode current. This difference in behavior suggests that the emitted electrons of the two peaks have very different origins and mechanisms. It is likely that the low-energy peak is due to electrons that have transited the *p*-AlGaN EBL by tunneling or percolative pathways towards the *p*-type surface [24,25]. Due to the sublinear increase in intensity shown by the high-energy peak we believe that the likely mechanism responsible for these hot electrons is a trap-assisted Auger recombination (TAAR) occurring due to the presence of the AlGaN EBL. TAAR is a well-documented nonradiative mechanism [26–31]. For electron-electron TAAR, an electron is captured from the conduction band to a trap state within the forbidden gap via concurrent generation of a second hot electron. A similar TAAR was observed in InGaN-based MBE grown QW LEDs and is the subject of forthcoming work [32,33]. It is reasonable that the number of traps that are available to participate in TAAR processes is finite in these high-quality materials, and it is expected that the integrated intensity of this peak should saturate with increased diode current as observed in Fig. 3(b).

We then measured (Figs. 4 and 5) the temperature dependent EDCs from forward biased LEDs in the intensity droop regime ($I = 25$ mA, corresponding to ∼20 A/cm^2, the onset of intensity droop being ∼3 A/cm^2). The EE spectra from the LED without an AlGaN EBL [Fig. 4(a)] showed the expected

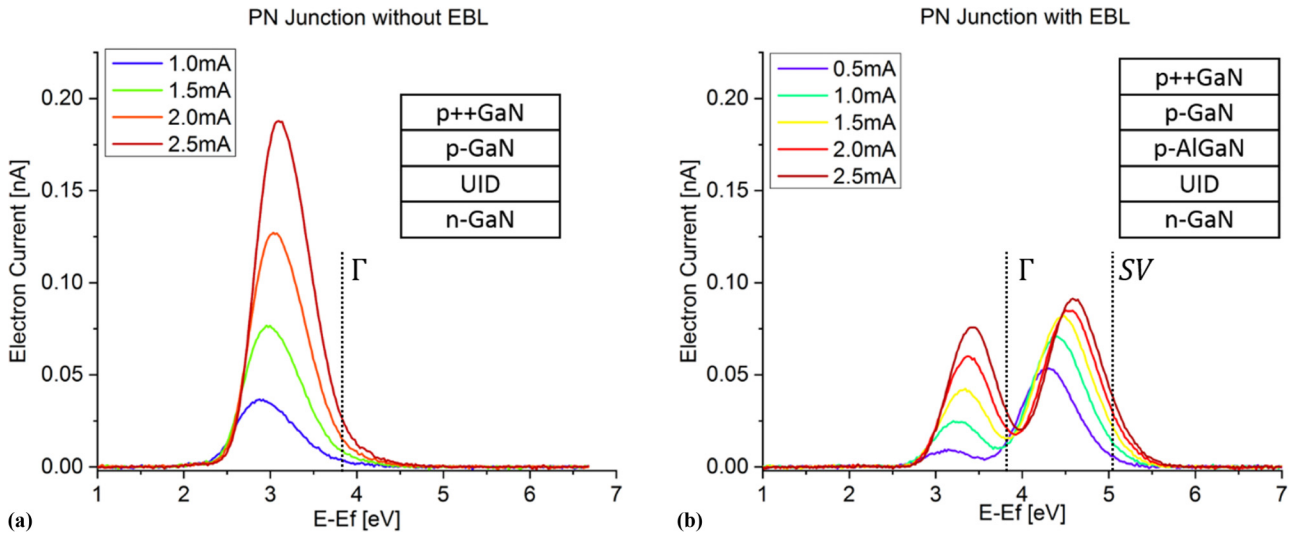

FIG. 3. (a) EDCs from *p-i-n* device with a single peak (Γ) with a high-energy threshold ∼3.7 eV. (b) EDCs from *p-i-n* + EBL device with two peaks (Γ and SV).

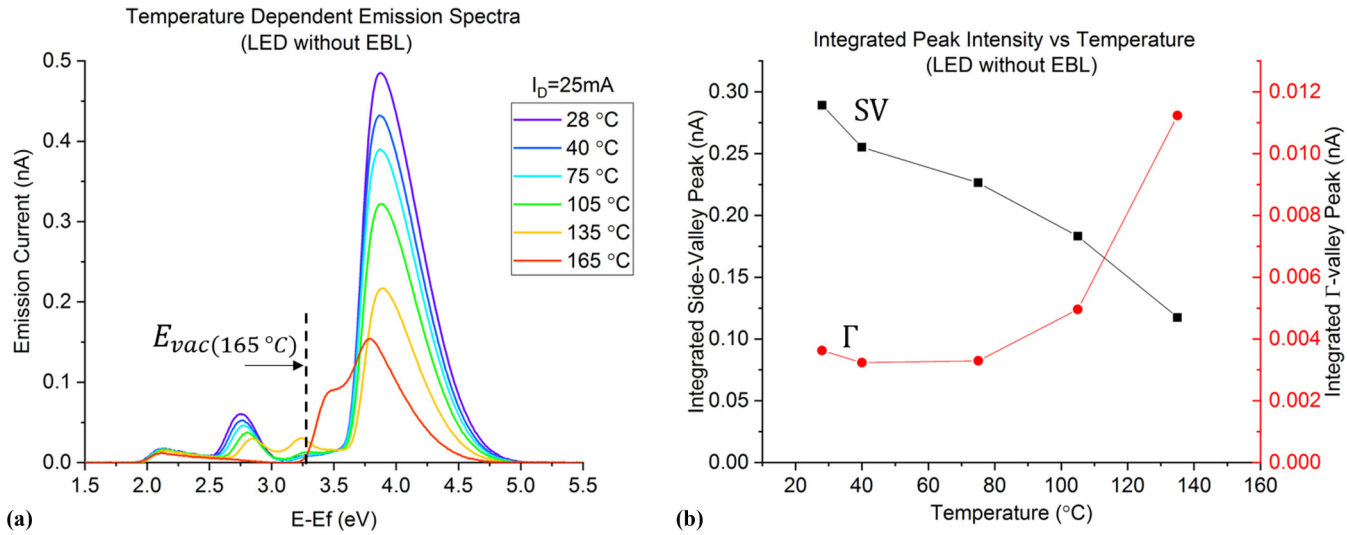

FIG. 4. (a) EDCs of an LED structure without AlGaN EBL, measured at 25 mA and varying temperature between 28–165 °C. (b) Integrals of the SV and Γ-valley peaks plotted as a function of temperature. The highest temperature datapoint for Γ valley is obscured from increase of GaN vacuum level preventing emission of the low-energy portion of the Γ-valley peak.

four peaks, two low-energy peaks due to photoemission from the *p*-contact metals, a mid-energy peak that aligned with the expected Γ-valley position, and a high-energy peak generated by interband Auger recombination in the LED active region [9,17]. Examination of the integrated intensity of the semiconductor emitted peaks [Fig. 4(b)], the mid-energy, Γ-valley peak intensity remained relatively constant at temperatures up to 75 °C. At temperatures above 75 °C, its intensity increased rapidly. Because the Γ-valley peak increase does not coincide with a corresponding, rapid decrease in SV emission it is unlikely this effect is due to intervalley scattering from the SV to the Γ valley [34]. The only mechanism explaining this increase in Γ-valley emission is an increase in electrons that have escaped [35] from the active region and ended up in the Γ valley of the *p*-GaN. The anticorrelation of Γ and SV peaks intensities is thus well explained from the increased backscattering of electrons from the SV with temperature [36].

Temperature dependent EES measurements from an LED that includes an AlGaN EBL again showed the expected four peaks and have some similarities to the LED without the EBL. The mid-energy, Γ-valley peak emission from this device is quasi constant up to 105 °C, with some increase between 75 and 105 °C most likely due to relaxation of SV electrons generated by an interband Auger, as in the LED without an EBL. This quasiconstancy of electrons generation in the *p* layer up to 105 °C shows that carrier escape cannot be the source of *intensity droop* present at 25 mA as this mechanism would vary strongly over such a temperature range. However, the Γ electron peak intensity increases rapidly above 130 °C, due to thermally activated carrier escape. Surprisingly, the SV

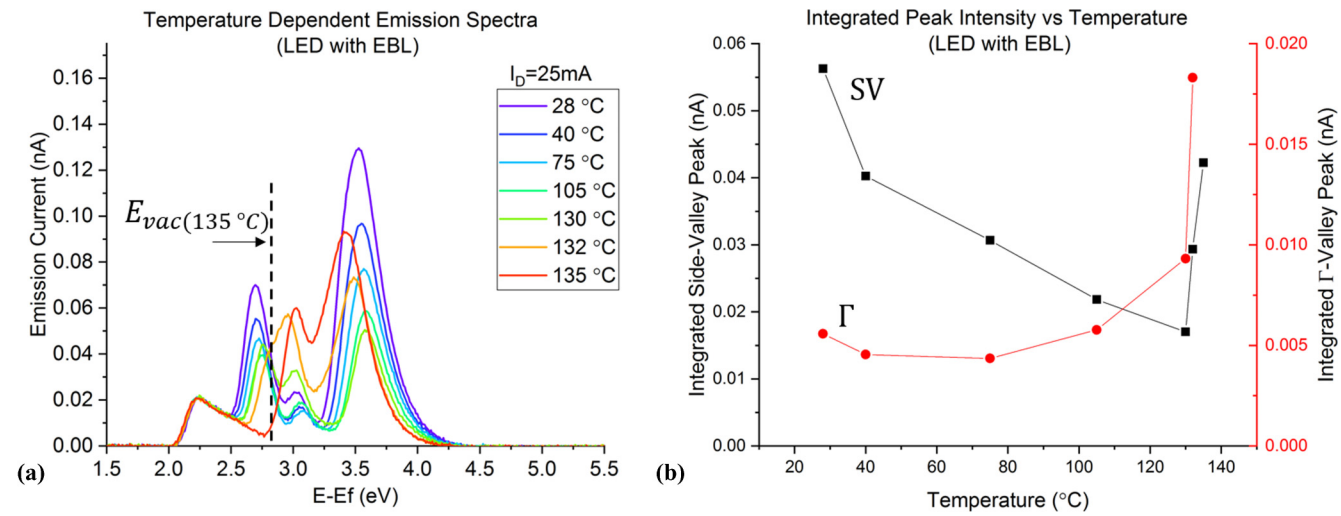

FIG. 5. (a) EDCs of an LED with EBL measured at 25 mA with varying temperatures (28–135 °C). Four peaks are visible, two low-energy, photoemission peaks form the *p*-contact metals and two higher energy, electroemission peaks from Γ and high-energy SV. (b) Integrated peak intensity of Γ and high-energy SV peaks showing that at temperatures above 130 °C increase in SV emission indicating supplemental hot-carrier generation due to EBL.

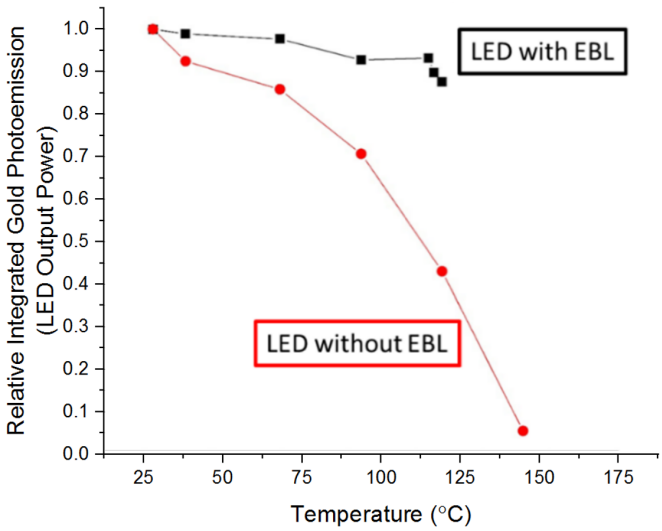

FIG. 6. Light-output power as measured by the integrated (gold) photoemission intensity for both LED structures injected at 25 mA.

integrated peak intensity also increases sharply at temperatures over 130 °C, an effect not present in devices without an AlGaN EBL when carrier escape sets in above 100 °C. We attribute the generation of additional hot electrons in the LED with an EBL operated at high temperatures to escaping electrons interacting with the *p*-AlGaN layer. By comparison with the high-energy peak observed in *p-i-n* + EBL experiments at 25 °C (Fig. 5), the appearance of SV electrons is here the *fingerprint* of electrons interacting with the EBL. The sharp increase in both Γ and SV electron intensities is thus due to thermally activated carrier escape, SV electrons being generated by the TAAR of the EBL, Γ electrons due to both passing through the EBL and relaxation from SV electrons [24,25].

A surprising result is the comparison of the intensities of the SV peak from LEDs with and without EBLs [Figs. 4(b) and 5(b)]. LEDs without an EBL emit ∼5× more hot electrons than LEDs with EBL before thermal escape sets in at 130 °C for the latter. As we expect similar interband Auger generation rates for LEDs with and without an EBL, we assume that the EBL may scatter hot electrons back into the active region due to quantum reflection of hot carriers from the SV conduction band discontinuities in the GaN/AlGaN/GaN heterostructure. This measured decrease in the SV emission for samples containing an AlGaN EBL is consistent across several devices. It shows that while some Γ electrons are able to pass through the EBL, the presence of the AlGaN heterostructure barrier may also mitigate some of the carrier losses due to interband Auger recombination in the QWs [37].

Finally, we compared the temperature dependence of the LED efficiencies, as measured by the metal photoemission integrated intensity (Fig. 6). LEDs that did not contain an AlGaN EBL showed a relatively large thermal droop, i.e., decrease in EL intensity, (∼30%) as temperature increased to 165 °C. Most of the decrease in electroluminescence occurs at temperatures above 75 °C in agreement with the carrier overshoot measured as an increased Γ-valley electron emission at these same temperatures [Fig. 4(b)]. EES-based thermal droop measurements from LEDs with an AlGaN EBL showed a much smaller electroluminescence decrease of only ∼5%, similar to other commercially produced LEDs [38]. Most of this decrease in electroluminescence occurred at temperatures above 130 °C, coinciding with the sudden increase in SV emission, likely due to TAAR, indicative of electrons hitting the EBL.

In conclusion, we have used EES to directly observe the generation of hot electrons in a semiconductor barrier heterostructure by the analysis of the energy distribution curves of electrons from electrically injected LEDs and *p-i-n* diodes. In both types of device, the presence of an AlGaN EBL provides a pathway for hot electron generation, likely through a TAAR process. For the LED with an EBL, the simultaneous appearance with increased temperature of hot electrons generated by EBL-induced TAAR and temperature droop unambiguously identifies thermal carrier escape as the mechanism for thermal droop for InGaN/GaN LEDs. The delayed appearance of carrier escape with temperature demonstrates the effectiveness of the AlGaN EBL at mitigating the loss of electroluminescence efficiency at elevated temperatures.

The authors would like to acknowledge Dr. Joo Won Choi from Seoul Viosys for providing commercially grown LEDs. This work was supported by the U.S. Department of Energy under the Office of Energy Efficiency & Renewable Energy (EERE) Award No. DE-EE0007096. Part of this work was performed in the UCSB Nanofabrication Facility.

[1] Z. Shen, M. E. Thompson, P. E. Burrows, V. Bulovic, S. R. Forrest, and D. M. McCarty, Jpn. J. Appl. Phys. **35**, L401 (1996).

[2] V. Bachmann, C. Ronda, and A. Meijerink, Chem. Mater. **21**, 2077 (2009).

[3] R. A. Street, Solid State Commun. **24**, 363 (1977).

[4] V. N. Abakumov, V. I. Perel, and I. N. Yassievich, *Nonradiative Recombination in Semiconductors* (Elsevier, Amsterdam, 1991).

[5] A. Alkauskas, Q. Yan, and C. G. Van de Walle, Phys. Rev. B **90**, 075202 (2014).

[6] C. De Santi, M. Meneghini, M. La Grassa, B. Galler, R. Zeisel, M. Goano, S. Dominici, M. Mandurrino, F. Bertazzi, D. Robidas, G. Meneghesso, and E. Zanoni, J. Appl. Phys. **119**, 094501 (2016).

[7] A. Nirschl, A. Gomez-Iglesias, M. Sabathil, G. Hartung, J. Off, and D. Bougeard, Phys. Status Solidi Appl. Mater. Sci. **211**, 2509 (2014).

[8] D. S. Meyaard, Q. Shan, Q. Dai, J. Cho, E. F. Schubert, M.-H. Kim, and C. Sone, Appl. Phys. Lett. **99**, 041112 (2011).

[9] J. Iveland, L. Martinelli, J. Peretti, J. S. Speck, and C. Weisbuch, Phys. Rev. Lett. **110**, 177406 (2013).

[10] A. David, M. J. Grundmann, J. F. Kaeding, N. F. Gardner, T. G. Mihopoulos, and M. R. Krames, Appl. Phys. Lett. **92**, 053502 (2008).
[11] A. David and M. J. Grundmann, Appl. Phys. Lett. **97**, 033501 (2010).
[12] C. K. Li, M. Piccardo, L. S. Lu, S. Mayboroda, L. Martinelli, J. Peretti, J. S. Speck, C. Weisbuch, M. Filoche, and Y. R. Wu, Phys. Rev. B **95**, 144206 (2017).
[13] Y. C. Shen, G. O. Mueller, S. Watanabe, N. F. Gardner, A. Munkholm, and M. R. Krames, Appl. Phys. Lett. **91**, 141101 (2007).
[14] O. E. Tereshchenko, D. Paget, P. Chiaradia, J. E. Bonnet, F. Wiame, and A. Taleb-lbrahimi, Appl. Phys. Lett. **82**, 4280 (2003).
[15] O. E. Tereshchenko, G. É. Shaibler, A. S. Yaroshevich, S. V. Shevelev, A. S. Terekhov, V. V. Lundin, E. E. Zavarin, and A. I. Besyul'kin, Phys. Solid State **46**, 1949 (2004).
[16] C. I. Wu and A. Kahn, Appl. Surf. Sci. **162**, 250 (2000).
[17] D. J. Myers, K. Gelžinyte, W. Y. Ho, J. Iveland, L. Martinelli, J. Peretti, C. Weisbuch, and J. S. Speck, J. Appl. Phys. **124**, 055703 (2018).
[18] J. Iveland, M. Piccardo, L. Martinelli, J. Peretti, J. W. Choi, N. Young, S. Nakamura, J. S. Speck, and C. Weisbuch, Appl. Phys. Lett. **105**, 052103 (2014).
[19] S. Wu, P. Geiser, J. Jun, J. Karpinski, and R. Sobolewski, in *Proceedings of the Conference on Lasers and Electro-Optics/Quantum Electronics and Laser Science and Photonic Applications Systems Technologies*, OSA Technical Digest Series (CD) (Optical Society of America, 2007), paper JThD29.
[20] S. Marcinkevičius, T. K. Uždavinys, H. M. Foronda, D. A. Cohen, C. Weisbuch, and J. S. Speck, Phys. Rev. B **94**, 235205 (2016).
[21] M. Piccardo, L. Martinelli, J. Iveland, N. Young, S. P. DenBaars, S. Nakamura, J. S. Speck, C. Weisbuch, and J. Peretti, Phys. Rev. B **89**, 235124 (2014).
[22] The difference in maximum temperatures for the various measurements reported in Figs. 2, 4, and 6 is due to the poor run-to-run reproducibility of the sequences of cesiation, temperature ramping, and measurement, full decesiation at high temperatures and recesiation. As partial decesiations occur at different temperatures when ramping up temperature, the maximum temperatures for which one obtains reliable peak intensity measurements are different. The maximum measurement temperatures were 165 and 135 °C for the LED without and with an EBL, respectively, due to the vacuum reaching the Γ peak.
[23] Z. Liu, F. Machuca, P. Pianetta, W. E. Spicer, and R. F. W. Pease, Appl. Phys. Lett. **85**, 1541 (2004).
[24] D. N. Nath, Z. C. Yang, C. Y. Lee, P. S. Park, Y. R. Wu, and S. Rajan, Appl. Phys. Lett. **103**, 022102 (2013).
[25] K. B. Lee, P. J. Parbrook, T. Wang, J. Bai, F. Ranalli, R. J. Airey, and G. Hill, J. Cryst. Growth **311**, 2857 (2009).
[26] P. T. Landsberg, D. A. Evans, and C. Rhys-Roberts, Proc. Phys. Soc. **83**, 325 (1964).
[27] A. Haug, Phys. Status Solidi **97**, 481 (1980).
[28] A. Haug, Appl. Phys. A **56**, 567 (1993).
[29] A. Hangleiter, Phys. Rev. Lett. **55**, 2976 (1985).
[30] A. Hangleiter, Phys. Rev. B **37**, 2594 (1988).
[31] V. B. Khalfin, M. V. Strikha, and I. N. Yassievich, Phys. Status Solidi **132**, 203 (1985).
[32] D. J. Myers, A. C. Espenlaub, E. C. Young, G. Gelinyte, L. Martinelli, J. Peretti, C. Weisbuch, and J. S. Speck (unpublished).
[33] A. C. Espenlaub, D. J. Myers, E. C. Young, S. Marcinkevičius, C. Weisbuch, and J. S. Speck (unpublished).
[34] One might contemplate both a temperature increase in interband Auger and increased backscattering from the SV, which would lead to the observation. However, this would also occur at the same temperature for the LED with EBL where the increase in Γ-valley emission [Fig. 5(b)] and droop (Fig. 6) occurs at quite a higher temperature.
[35] From now on we do not consider further overshoot as a droop Mechanism as it is basically not temperature dependent as observed here, and only consider thermal escape.
[36] J. Sjakste, K. Tanimura, G. Barbarino, L. Perfetti, and N. Vast, J. Phys.: Condens. Matter **30**, 353001 (2018).
[37] M. Deppner, F. Römer, and B. Witzigmann, Phys. Status Solidi (RRL) **6**, 418 (2012).
[38] See, e.g., Lumileds, "Luxeon v" Datasheet (2019); Nichia, "NF2W757GT-V3F1" Datasheet (2018); Cree, "XLamp XD16 LEDs" Datasheet (2018).